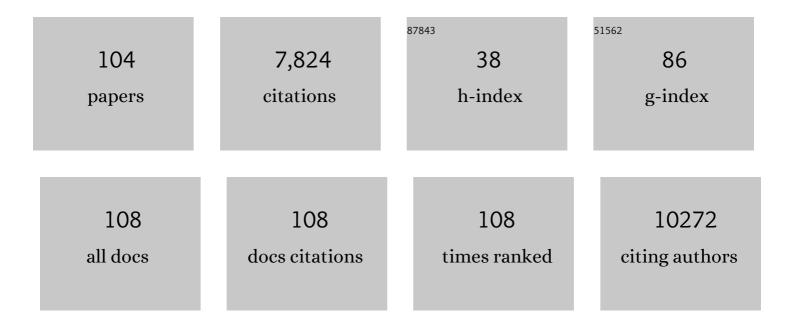
List of Publications by Year in descending order

Source: https://exaly.com/author-pdf/4584257/publications.pdf Version: 2024-02-01



#	Article	IF	CITATIONS
1	Fast fragment- and compound-screening pipeline at the Swiss Light Source. Acta Crystallographica Section D: Structural Biology, 2022, 78, 328-336.	1.1	11
2	AgeR deletion decreases soluble fms-like tyrosine kinase 1 production and improves post-ischemic angiogenesis in uremic mice. Angiogenesis, 2021, 24, 47-55.	3.7	1
3	Cu ²⁺ -binding to S100B triggers polymerization of disulfide cross-linked tetramers with enhanced chaperone activity against amyloid-l² aggregation. Chemical Communications, 2021, 57, 379-382.	2.2	6
4	A Sodium-Translocating Module Linking Succinate Production to Formation of Membrane Potential in Prevotella bryantii. Applied and Environmental Microbiology, 2021, 87, e0121121.	1.4	10
5	Dynamic interactions and Ca2+-binding modulate the holdase-type chaperone activity of S100B preventing tau aggregation and seeding. Nature Communications, 2021, 12, 6292.	5.8	10
6	Central Carbon Metabolism, Sodium-Motive Electron Transfer, and Ammonium Formation by the Vaginal Pathogen Prevotella bivia. International Journal of Molecular Sciences, 2021, 22, 11925.	1.8	5
7	Impact of Na ⁺ -Translocating NADH:Quinone Oxidoreductase on Iron Uptake and <i>nqrM</i> Expression in Vibrio cholerae. Journal of Bacteriology, 2020, 202, .	1.0	4
8	Prothrombin is a binding partner of the human receptor of advanced glycation end products. Journal of Biological Chemistry, 2020, 295, 12498-12511.	1.6	5
9	Receptor for Advanced Glycation End Products is Involved in Platelet Hyperactivation and Arterial Thrombosis during Chronic Kidney Disease. Thrombosis and Haemostasis, 2020, 120, 1300-1312.	1.8	5
10	Concise Synthesis of 1,4â€Benzoquinoneâ€Based Natural Products as Mitochondrial Complex I Substrates and Substrateâ€Based Inhibitors. ChemMedChem, 2020, 15, 2491-2499.	1.6	2
11	Anoxic cell rupture of Prevotella bryantii by high-pressure homogenization protects the Na+-translocating NADH:quinone oxidoreductase from oxidative damage. Archives of Microbiology, 2020, 202, 1263-1266.	1.0	3
12	Cryo-EM structure of a transthyretin-derived amyloid fibril from a patient with hereditary ATTR amyloidosis. Nature Communications, 2019, 10, 5008.	5.8	127
13	Altered Notch Signaling in Dowling-Degos Disease: Additional Mutations in POGLUT1 and Further Insights into Disease Pathogenesis. Journal of Investigative Dermatology, 2019, 139, 960-964.	0.3	15
14	Respiratory Membrane Protein Complexes Convert Chemical Energy. Sub-Cellular Biochemistry, 2019, 92, 301-335.	1.0	5
15	Cryo-EM structure of a light chain-derived amyloid fibril from a patient with systemic AL amyloidosis. Nature Communications, 2019, 10, 1103.	5.8	120
16	Receptor for advanced glycation end products: a key molecule in the genesis of chronic kidney disease vascular calcification and a potential modulator of sodium phosphate co-transporter PIT-1 expression. Nephrology Dialysis Transplantation, 2019, 34, 2018-2030.	0.4	28
17	How USP 18 deals with ISG 15â€modified proteins: structural basis for the specificity of the protease. FEBS Journal, 2018, 285, 1024-1029.	2.2	17
18	Vibrio natriegens as Host for Expression of Multisubunit Membrane Protein Complexes. Frontiers in Microbiology, 2018, 9, 2537.	1.5	33

#	Article	IF	CITATIONS
19	The neuronal S100B protein is a calcium-tuned suppressor of amyloid-β aggregation. Science Advances, 2018, 4, eaaq1702.	4.7	49
20	USP18 â \in " a multifunctional component in the interferon response. Bioscience Reports, 2018, 38, .	1.1	61
21	A capture method based on the VC1 domain reveals new binding properties of the human receptor for advanced glycation end products (RAGE). Redox Biology, 2017, 11, 275-285.	3.9	16
22	Structural basis of the specificity of USP18 toward ISC15. Nature Structural and Molecular Biology, 2017, 24, 270-278.	3.6	85
23	A miniaturized assay for kinetic characterization of the Na+-translocating NADH:ubiquinone oxidoreductase from Vibrio cholerae. Analytical Biochemistry, 2017, 537, 56-59.	1.1	Ο
24	Strong pH dependence of coupling efficiency of the Na ⁺ – translocating NADH:quinone oxidoreductase (Na ⁺ -NQR) of <i>Vibrio cholerae</i> . Biological Chemistry, 2017, 398, 251-260.	1.2	9
25	Sodium as Coupling Cation in Respiratory Energy Conversion. Metal lons in Life Sciences, 2016, 16, 349-390.	2.8	3
26	The Mouse-Specific Splice Variant mRAGE_v4 Encodes a Membrane-Bound RAGE That Is Resistant to Shedding and Does Not Contribute to the Production of Soluble RAGE. PLoS ONE, 2016, 11, e0153832.	1.1	6
27	Identification of a novel mutation in <i>RIPK4</i> in a kindred with phenotypic features of Bartsocasâ€Papas and CHAND syndromes. American Journal of Medical Genetics, Part A, 2015, 167, 2555-2562.	0.7	11
28	Sulfate to go. Science, 2015, 350, 1476-1477.	6.0	5
29	Pathogenicity of POFUT1 in Dowling-Degos Disease: Additional Mutations and Clinical Overlap with Reticulate Acropigmentation of Kitamura. Journal of Investigative Dermatology, 2015, 135, 615-618.	0.3	25
30	An improved expression system for the VC1 ligand binding domain of the receptor for advanced glycation end products in Pichia pastoris. Protein Expression and Purification, 2015, 114, 48-57.	0.6	8
31	The structure of Na+-translocating of NADH:ubiquinone oxidoreductase of Vibrio cholerae: implications on coupling between electron transfer and Na+ transport. Biological Chemistry, 2015, 396, 1015-1030.	1.2	27
32	<scp>USP</scp> 18 lack in microglia causes destructive interferonopathy of the mouse brain. EMBO Journal, 2015, 34, 1612-1629.	3.5	178
33	The Receptor for Advanced Clycation End-Products (RAGE) Is Only Present in Mammals, and Belongs to a Family of Cell Adhesion Molecules (CAMs). PLoS ONE, 2014, 9, e86903.	1.1	115
34	Structure of the V. cholerae Na+-pumping NADH:quinone oxidoreductase. Nature, 2014, 516, 62-67.	13.7	107
35	Structural Heterogeneity and Bioimaging of S100 Amyloid Assemblies. , 2014, , 197-212.		4
36	Central role of the Na+-translocating NADH:quinone oxidoreductase (Na+-NQR) in sodium bioenergetics of Vibrio cholerae. Biological Chemistry, 2014, 395, 1389-1399.	1.2	29

GüNTER FRITZ

#	Article	IF	CITATIONS
37	Molecular characterization of ubiquitinâ€specific protease 18 reveals substrate specificity for interferonâ€stimulated gene 15. FEBS Journal, 2014, 281, 1918-1928.	2.2	48
38	Crystallization and preliminary analysis of the NqrA and NqrC subunits of the Na+-translocating NADH:ubiquinone oxidoreductase fromVibrio cholerae. Acta Crystallographica Section F, Structural Biology Communications, 2014, 70, 987-992.	0.4	13
39	Mutations in POGLUT1, Encoding Protein O-Glucosyltransferase 1, Cause Autosomal-Dominant Dowling-Degos Disease. American Journal of Human Genetics, 2014, 94, 135-143.	2.6	136
40	RAGE regulation and signaling in inflammation and beyond. Journal of Leukocyte Biology, 2013, 94, 55-68.	1.5	336
41	1H, 13C, and 15N resonance assignments of the second immunoglobulin domain of neurolin from Carassius auratus. Biomolecular NMR Assignments, 2013, 7, 65-67.	0.4	0
42	Molecular basis for manganese sequestration by calprotectin and roles in the innate immune response to invading bacterial pathogens. Proceedings of the National Academy of Sciences of the United States of America, 2013, 110, 3841-3846.	3.3	325
43	Microglia emerge from erythromyeloid precursors via Pu.1- and Irf8-dependent pathways. Nature Neuroscience, 2013, 16, 273-280.	7.1	1,121
44	Conserving energy with sulfate around 100 °C – structure and mechanism of key metal enzymes in hyperthermophilic Archaeoglobus fulgidus. Metallomics, 2013, 5, 302.	1.0	26
45	Intrinsically Disordered and Aggregation Prone Regions Underlie β-Aggregation in S100 Proteins. PLoS ONE, 2013, 8, e76629.	1.1	22
46	X-ray Structural Analysis of S100 Proteins. Methods in Molecular Biology, 2013, 963, 87-97.	0.4	3
47	HMGB1 conveys immunosuppressive characteristics on regulatory and conventional T cells. International Immunology, 2012, 24, 485-494.	1.8	85
48	Analysis of S100 Oligomers and Amyloids. Methods in Molecular Biology, 2012, 849, 373-386.	0.4	23
49	Formin mDia1 Mediates Vascular Remodeling via Integration of Oxidative and Signal Transduction Pathways. Circulation Research, 2012, 110, 1279-1293.	2.0	78
50	S100A6 Amyloid Fibril Formation Is Calcium-modulated and Enhances Superoxide Dismutase-1 (SOD1) Aggregation. Journal of Biological Chemistry, 2012, 287, 42233-42242.	1.6	36
51	High yield expression of catalytically active USP18 (UBP43) using a Trigger Factor fusion system. BMC Biotechnology, 2012, 12, 56.	1.7	14
52	A multimodal RAGE-specific inhibitor reduces amyloid β–mediated brain disorder in a mouse model of Alzheimer disease. Journal of Clinical Investigation, 2012, 122, 1377-1392.	3.9	507
53	The Catalytic Redox Activity of Prion Protein–Cu ^{II} is Controlled by Metal Exchange with the Zn ^{II} –Thiolate Clusters of Zn ₇ Metallothioneinâ€3. ChemBioChem, 2012, 13, 1261-1265.	1.3	18
54	The structure of Ca ²⁺ â€loaded S100A2 at 1.3â€Ã resolution. FEBS Journal, 2012, 279, 1799-1810	. 2.2	9

4

#	Article	IF	CITATIONS
55	Low-resolution structure determination of Na+-translocating NADH:ubiquinone oxidoreductase fromVibrio choleraebyab initiophasing and electron microscopy. Acta Crystallographica Section D: Biological Crystallography, 2012, 68, 724-731.	2.5	4
56	Pattern Recognition with a Fibril-Specific Antibody Fragment Reveals the Surface Variability of Natural Amyloid Fibrils. Journal of Molecular Biology, 2011, 408, 529-540.	2.0	34
57	RAGE: a single receptor fits multiple ligands. Trends in Biochemical Sciences, 2011, 36, 625-632.	3.7	267
58	The crystal structures of human S100B in the zinc- and calcium-loaded state at three pH values reveal zinc ligand swapping. Biochimica Et Biophysica Acta - Molecular Cell Research, 2011, 1813, 1083-1091.	1.9	43
59	Structural Basis for Ligand Recognition and Activation of RAGE. Structure, 2010, 18, 1342-1352.	1.6	195
60	Crystallization and calcium/sulfur SAD phasing of the human EF-hand protein S100A2. Acta Crystallographica Section F: Structural Biology Communications, 2010, 66, 1032-1036.	0.7	6
61	Crystallization of the Na+-translocating NADH:quinone oxidoreductase fromVibrio cholerae. Acta Crystallographica Section F: Structural Biology Communications, 2010, 66, 1677-1679.	0.7	16
62	Natural and amyloid selfâ€assembly of S100 proteins: structural basis of functional diversity. FEBS Journal, 2010, 277, 4578-4590.	2.2	115
63	The Family of S100 Cell Signaling Proteins. , 2010, , 983-993.		3
64	Localization and Function of the Membrane-bound Riboflavin in the Na+-translocating NADH:Quinone Oxidoreductase (Na+-NQR) from Vibrio cholerae. Journal of Biological Chemistry, 2010, 285, 27088-27099.	1.6	36
65	Generation and characterization of a novel, permanently active S100P mutant. Biochimica Et Biophysica Acta - Molecular Cell Research, 2009, 1793, 1078-1085.	1.9	7
66	Binding of S100 proteins to RAGE: An update. Biochimica Et Biophysica Acta - Molecular Cell Research, 2009, 1793, 993-1007.	1.9	413
67	Metal ions modulate the folding and stability of the tumor suppressor protein S100A2. FEBS Journal, 2009, 276, 1776-1786.	2.2	29
68	The Na+-translocating NADH:quinone oxidoreductase (Na+-NQR) from Vibrio cholerae enhances insertion of FeS in overproduced NqrF subunit. Journal of Inorganic Biochemistry, 2008, 102, 1366-1372.	1.5	5
69	V domain of RAGE interacts with AGEs on prostate carcinoma cells. Prostate, 2008, 68, 748-758.	1.2	45
70	Oxidant-induced formation of a neutral flavosemiquinone in the Na+-translocating NADH:Quinone oxidoreductase (Na+-NQR) from Vibrio cholerae. Biochimica Et Biophysica Acta - Bioenergetics, 2008, 1777, 696-702.	0.5	26
71	The deletion of amino acids 114–121 in the TM1 domain of mouse prion protein stabilizes its conformation but does not affect the overall structure. Biochimica Et Biophysica Acta - Molecular Cell Research, 2008, 1783, 1076-1084.	1.9	3
72	S4.28 Crystal structure of the NADH-oxidizing FAD domain from the Na+-translocating NADH:quinone oxidoreductase (Na+-NQR). Biochimica Et Biophysica Acta - Bioenergetics, 2008, 1777, S39.	0.5	2

GüNTER FRITZ

4

#	Article	IF	CITATIONS
73	Crystal Structure of Ca2+-Free S100A2 at 1.6-Ã Resolution. Journal of Molecular Biology, 2008, 378, 933-942.	2.0	30
74	Expression and purification of neurolin immunoglobulin domain 2 from Carrassius auratus (goldfish) in Escherichia coli. Protein Expression and Purification, 2008, 59, 47-54.	0.6	6
75	Living on Sulfate: Three-Dimensional Structure and Spectroscopy of Adenosine 5´-Phosphosulfate Reductase and Dissimilatory Sulfite Reductase. , 2008, , 13-23.		1
76	S100B and S100A6 Differentially Modulate Cell Survival by Interacting with Distinct RAGE (Receptor) Tj ETQq0 0 2007, 282, 31317-31331.	0 rgBT /C 1.6	overlock 10 Tf 234
77	Quinone Reduction by the Na + -Translocating NADH Dehydrogenase Promotes Extracellular Superoxide Production in Vibrio cholerae. Journal of Bacteriology, 2007, 189, 3902-3908.	1.0	37
78	The Extracellular Region of the Receptor for Advanced Glycation End Products Is Composed of Two Independent Structural Unitsâ€. Biochemistry, 2007, 46, 6957-6970.	1.2	156
79	Structural and functional insights into RAGE activation by multimeric S100B. EMBO Journal, 2007, 26, 3868-3878.	3.5	219
80	Implications on zinc binding to S100A2. Biochimica Et Biophysica Acta - Molecular Cell Research, 2007, 1773, 457-470.	1.9	49
81	Reaction Mechanism of the Ironâ^'Sulfur Flavoenzyme Adenosine-5â€~-Phosphosulfate Reductase Based on the Structural Characterization of Different Enzymatic Statesâ€,‡. Biochemistry, 2006, 45, 2960-2967.	1.2	38
82	Expression and purification of the soluble isoform of human receptor for advanced glycation end products (sRAGE) from Pichia pastoris. Biochemical and Biophysical Research Communications, 2006, 347, 4-11.	1.0	31
83	Crystallization of the NADH-oxidizing domain of the Na+-translocating NADH:ubiquinone oxidoreductase fromVibrio cholerae. Acta Crystallographica Section F: Structural Biology Communications, 2006, 62, 110-112.	0.7	11
84	Purification and crystallization of the human EF-hand tumour suppressor protein S100A2. Acta Crystallographica Section F: Structural Biology Communications, 2006, 62, 1120-1123.	0.7	6
85	Electron spin relaxation of copper(II) complexes in glassy solution between 10 and 120K. Journal of Magnetic Resonance, 2006, 179, 92-104.	1.2	48
86	Purification, crystallization and preliminary X-ray diffraction studies on human Ca2+-binding protein S100B. Acta Crystallographica Section F: Structural Biology Communications, 2005, 61, 673-675.	0.7	16
87	NADH Oxidation by the Na+-translocating NADH:Quinone Oxidoreductase from Vibrio cholerae. Journal of Biological Chemistry, 2004, 279, 21349-21355.	1.6	51
88	S100 proteins in mouse and man: from evolution to function and pathology (including an update of) Tj ETQq0 0	0 rgBT /O	verlggk 10 Tf
89	Alzheimer β-Amyloid Homodimers Facilitate Aβ Fibrillization and the Generation of Conformational Antibodies. Journal of Biological Chemistry, 2003, 278, 35317-35324.	1.6	64

90 The Family of S100 Cell Signaling Proteins. , 2003, , 87-93.

6

#	Article	IF	CITATIONS
91	The Function of the [4Fe-4S] Clusters and FAD in Bacterial and Archaeal Adenylylsulfate Reductases. Journal of Biological Chemistry, 2002, 277, 26066-26073.	1.6	47
92	The Crystal Structure of Metal-free Human EF-hand Protein S100A3 at 1.7-Ã Resolution. Journal of Biological Chemistry, 2002, 277, 33092-33098.	1.6	50
93	Structure of adenylylsulfate reductase from the hyperthermophilic Archaeoglobus fulgidus at 1.6-A resolution. Proceedings of the National Academy of Sciences of the United States of America, 2002, 99, 1836-1841.	3.3	78
94	The Presence of an Iron-Sulfur Cluster in Adenosine 5′-Phosphosulfate Reductase Separates Organisms Utilizing Adenosine 5′-Phosphosulfate and Phosphoadenosine 5′-Phosphosulfate for Sulfate Assimilation. Journal of Biological Chemistry, 2002, 277, 21786-21791.	1.6	96
95	Metal-free MIRAS phasing: structure of apo-S100A3. Acta Crystallographica Section D: Biological Crystallography, 2002, 58, 1255-1261.	2.5	16
96	Inactivation of the Na+-translocating NADH:ubiquinone oxidoreductase fromVibrio alginolyticusby reactive oxygen species. FEBS Journal, 2002, 269, 1287-1292.	0.2	6
97	S100 proteins structure functions and pathology. Frontiers in Bioscience - Landmark, 2002, 7, d1356-1368.	3.0	327
98	Three-Dimensional Structure of the Nonaheme CytochromecfromDesulfovibrio desulfuricansEssex in the Fe(III) State at 1.89 à Resolutionâ€,‡. Biochemistry, 2001, 40, 1308-1316.	1.2	27
99	Nonaheme Cytochromec, a New Physiological Electron Acceptor for [Ni,Fe] Hydrogenase in the Sulfate-Reducing BacteriumDesulfovibrio desulfuricansEssex:Â Primary Sequence, Molecular Parameters, and Redox Propertiesâ€. Biochemistry, 2001, 40, 1317-1324.	1.2	27
100	Spectroscopic investigation and determination of reactivity and structure of the tetraheme cytochromec3fromDesulfovibrio desulfuricansEssex 6. FEBS Journal, 2001, 268, 3028-3035.	0.2	27
101	Plant Adenosine 5′-Phosphosulfate Reductase Is a Novel Iron-Sulfur Protein. Journal of Biological Chemistry, 2001, 276, 42881-42886.	1.6	77
102	Crystallization and preliminary X-ray analysis of adenylylsulfate reductase fromArchaeoglobus fulgidus. Acta Crystallographica Section D: Biological Crystallography, 2000, 56, 1673-1675.	2.5	5
103	Adenylylsulfate reductases from archaea and bacteria are 1:1 αβ-heterodimeric iron-sulfur flavoenzymes - high similarity of molecular properties emphasizes their central role in sulfur metabolism. FEBS Letters, 2000, 473, 63-66.	1.3	47
104	Probing the structure of the human Ca2+- and Zn2+-binding protein S100A3: spectroscopic investigations of its transition metal ion complexes, and three-dimensional structural model. Biochimica Et Biophysica Acta - Molecular Cell Research, 1998, 1448, 264-276.	1.9	38